



# The thermal width of heavy quarkonia moving in quark–gluon plasma

Taesoo Song<sup>a,\*</sup>, Yongjae Park<sup>a</sup>, Su Houn Lee<sup>a</sup>, Cheuk-Yin Wong<sup>b,c</sup>

<sup>a</sup> Institute of Physics and Applied Physics, Yonsei University, Seoul 120-749, South Korea

<sup>b</sup> Physics Division, Oak Ridge National Laboratory, Oak Ridge, TN 37830, USA

<sup>c</sup> Department of Physics, University of Tennessee, Knoxville, TN 37996, USA

Received 10 September 2007; received in revised form 23 October 2007; accepted 27 November 2007

Available online 5 December 2007

Editor: J.-P. Blaizot

## Abstract

The velocity dependence of the thermal width of heavy quarkonia traveling with respect to the quark–gluon plasma is calculated up to the NLO in perturbative QCD. At the LO, the width decreases with increasing speed, whereas at the NLO it increases with a magnitude approximately proportional to the expectation value of the relative velocity between the quarkonium and a parton in thermal equilibrium. Such an asymptotic behavior is due to the NLO dissociation cross section converging to a nonvanishing value in the high energy limit.

© 2007 Elsevier B.V. All rights reserved.

PACS: 13.20.He; 14.20.Lq

Keywords: Quark–gluon plasma;  $J/\psi$  suppression; Heavy quarkonia; Perturbative QCD; Dissociation cross section; Thermal width

## 1. Introduction

Using arguments based on the contraction of the Debye screening length in quark–gluon plasma (QGP), Matsui and Satz [1] suggested  $J/\psi$  suppression to be a signature of the formation of QGP in the early stages of a heavy ion collision. Indeed measurements at past SPS data [2] showed nontrivial suppression patterns that could be consistent with the original prediction. However, recent lattice calculations show that  $J/\psi$  will survive past the critical temperature  $T_c$  for the phase transition [3–7] up to about  $1.6 T_c$ , while  $\chi_c$  and  $\psi'$  will dissolve above  $T_c$ . These findings suggest that a possible mechanisms for  $J/\psi$  suppression could be the disappearance of feedbacks from the  $\chi_c$  and  $\psi'$ , together with the hadronic matter effects, such as the nuclear absorption, the interactions with comovers, and the shadowing effect [8,9]. Using a more precise determination of the cold nuclear matter absorption cross section of charmonium through p–A collisions [10], it was found that such

a feed down suppression scenario was indeed favored in results from semi-central Pb–Pb collisions [11] and from central In–In collisions at 158 GeV/nucleon [12].

Phenomenologically, the statistical hadronization model [13–17] applied to the charmonium production [18] appears to be compatible with RHIC data [19,20]. In a kinetic model, the charmonium is produced in the whole temporal evolution of the QGP [21,22]. Further tests at LHC will discriminate between various pictures, and a unified picture is expected to emerge.

But before a simplified picture of  $J/\psi$  suppression can be adopted, detailed properties of  $J/\psi$  above  $T_c$  have to be investigated. Unfortunately, the present lattice calculations based on maximum entropy method still have poor resolution, and is not able to reliably determine the thermal width or possible mass shift above  $T_c$  [4,5]. However, there are several recent works that can supplement the lattice calculation. A recent QCD sum rule calculation using the running coupling constant and the gluon condensates extracted from a recent lattice data shows that the width of  $J/\psi$  may be broadened or the mass reduced just over  $T_c$  [23], which is consistent with results from AdS/QCD [24]. In another recent work, the Debye screening length in the  $J/\psi$  moving with respect to QGP was calculated in AdS/QCD [25]. In addition, the spectral functions of heavy

\* Corresponding author.

E-mail addresses: songtsoo@yonsei.ac.kr (T. Song), sfy@yonsei.ac.kr (Y. Park), suhoun@phya.yonsei.ac.kr (S.H. Lee), cyw@ornl.gov (C.-Y. Wong).

quarkonia were extracted from the imaginary part of Green functions obtained from potentials fitted to lattice data [26–29]. In another work, the thermal width of  $J/\psi$  was investigated using perturbative QCD up to the NLO [30]. The LO perturbative QCD calculation for the heavy quarkonium dissociation was invented by Peskin and Bhanot [31,32] more than 20 years ago. Later, one of us rederived the LO result using Bethe–Salpeter amplitude [33], which was further used to calculate the NLO results [34]. In that work, the bound state of quarkonium was described by Bethe–Salpeter amplitude, and the perturbative QCD method was applied to calculate the decay process. The binding energy of the quarkonium and its radius were obtained by solving the Schrödinger equation with the potential energy extracted from the lattice QCD calculation [35]. At the NLO, it was found that the thermal width of  $J/\psi$  increases as temperature increases, while it decreases in the LO. Moreover, the total width was found to grow to more than 250 MeV at  $1.4T_c$ , assuming the thermal quark–gluon masses to be around 400 MeV. If the thermal width is so large, the  $J/\psi$  initially formed at  $1.6T_c$ , will be dissociated immediately and not be able to escape the quark–gluon plasma until it cools down further to near  $T_c$ .

Another important aspect to be considered in a realistic heavy ion collision is the velocity of the  $J/\psi$  with respect to the QGP. In particular, at LHC, more energetic heavy quarkonia are expected to be produced and absorbed. Previously the Debye screening length between a heavy quark and a heavy anti-quark pair moving with respect to the QGP was calculated in a kinetic theory approach [36]. It was found that the Debye screening length becomes shorter as the velocity increases, because the parton density enhances in the heavy quarkonium rest frame [36,37]. Recently, the screening length was investigated in an AdS/CFT calculation [25,38], where it was found to be approximately proportional to  $[1 - v^2]^{1/4}$ ,  $v$  being the velocity of  $J/\psi$  with respect to the QGP. But whether AdS/CFT calculations represents real QCD phenomena still remain controversial. Therefore, in this work, we will extend a previous NLO perturbative QCD calculation for the thermal width of a quarkonium at rest [30] to that of a quarkonium moving with respect to the QGP. The works mentioned above [25,36–38] anticipated the shortening of the Debye screening length when the heavy quark and anti-quark pair moves in the quark–gluon matter or equivalently when the matter is boosted, which may be called as the change of static properties. On the other hand, our results provide another component of the change through the thermal width of the quarkonia as it moves through the matter. This may be called as the change of dynamical properties. The shortening of Debye screening length means the radius and the binding energy of heavy quarkonia should change as it moves through the matter. However, in this work, the radius and the binding energy of static quarkonia are used for the purpose of investigating the change of a purely dynamical property. We find that at the LO, the width decreases with increasing  $v$ , which is caused by the vanishing of the dissociation cross section of the quarkonium by an energetic gluon. However, at the NLO the thermal width increases with  $v$ . This is due to the nonvanishing asymptotic cross section between the quarkonium and an energetic parton at the NLO, which for the Coulomb wave func-

tion of the quarkonium scales as the square of the Bohr radius. In Section 2, we briefly review formulas used throughout this Letter. In Section 3, we apply these formulas to  $J/\psi$  and  $\Upsilon$ . Some discussions are given in Section 4. In Appendix A, we derive the asymptotic form of the dissociation cross section of a quarkonium in the high energy limit.

## 2. Thermal width of a heavy quarkonium in pQCD

The width of a hadron in the vacuum comes from its spontaneous decay. On the other hand, its thermal width results from its interactions with the surrounding thermal particles. This thermal width of a quarkonium moving with velocity  $\beta$  in the medium is defined as

$$\Gamma_\beta^{\text{eff}} = d_p \int \frac{d^3k}{(2\pi)^3} n(k_0) v_{\text{rel}}(\beta) \sigma(k, \beta), \quad (1)$$

where  $d_p$  is the degeneracy factor,  $n(k_0)$  is the distribution function of the thermal particle,  $v_{\text{rel}}$  the relative velocity between decaying particle and the thermal particle, and  $\sigma(k, \beta)$  their energy-dependent elementary dissociation cross section. Because we are interested in the decays of heavy quarkonia in the quark–gluon plasma, the decaying particle is a heavy quarkonium and the thermal particles are light quarks and gluons. In this work, we considered only three light flavors. The dissociation cross section can be written as

$$\sigma(k, \beta) = \frac{1}{4v_{\text{rel}}(\beta) E_\Phi(\beta) E_p(k)} \int d(\text{p.s.}) |\bar{M}|^2. \quad (2)$$

The first factor on the right side is the inverse of initial flux.  $E_\Phi(\beta)$ ,  $E_p(k)$  are the energies of a quarkonium and a parton respectively. p.s. means phase space of final states, and  $\bar{M}$  is the spin-averaged invariant amplitude. The invariant amplitudes for the decay of a quarkonium by partons are listed in [30,34]. Substituting Eq. (2) into Eq. (1) we find,

$$\begin{aligned} \Gamma_\beta^{\text{eff}} &= d_p \int \frac{d^3k}{(2\pi)^3} \frac{n(k \cdot u)}{4E_\Phi(\beta) E_p} \int d(\text{p.s.}) |\bar{M}|^2 \\ &= \frac{d_p}{2E_\Phi(\beta)} \int \frac{d^4k}{(2\pi)^3} \frac{\delta^+(k^2 - m_p^2)}{e^{k \cdot u/T} \pm 1} \int d(\text{p.s.}) |\bar{M}|^2. \end{aligned} \quad (3)$$

Here the positive sign in the denominator is for a fermion and the negative sign for a boson medium. The function  $\delta^+$  means only positive energy is allowed, and  $u$  is the four velocity of the thermal bath, hereafter called the Lab frame. In the Lab frame,  $u = (1, 0, 0, 0)$ , whereas in the quarkonium rest frame,  $u = (1 - \beta^2)^{-1/2} (1, 0, 0, -\beta)$ . In the second equality of Eq. (3), all factors except  $E_\Phi(\beta)$  are Lorentz invariant. In fact, because  $E_\Phi = \gamma m_\Phi$ , where  $\gamma = 1/\sqrt{1 - \beta^2}$  and  $m_\Phi$  is the mass of a quarkonium,  $\gamma \Gamma_\beta^{\text{eff}}$  is also Lorentz invariant quantity, and we have

$$\gamma \Gamma_\beta^{\text{eff}} = \gamma \Gamma_{\text{Lab}}^{\text{eff}} = \Gamma_{\text{quarkonium rest frame}}^{\text{eff}}, \quad (4)$$

where  $\Gamma_{\text{quarkonium rest frame}}^{\text{eff}}$  is calculated in the rest frame of the quarkonium with a moving medium. This relation just reflects time dilation.

### 3. The thermal width of moving $J/\psi$ and $\Upsilon$ in QGP

We now apply the preceding formulas to calculate the thermal width of the  $J/\psi$  and the  $\Upsilon$ . All calculation will be performed in the Lab frame, and  $\Gamma$  will be used to represent  $\Gamma_{\text{Lab}}^{\text{eff}}$  from now on. The degeneracy factor  $d_p$  in Eq. (1) is set to 16 for the gluons and to 36 for the quarks. For numerical purpose in these calculations, the  $T_c$  value is taken to be 170 MeV. The figures in the upper panel of Fig. 1 show the variation of the thermal width  $\Gamma$  of  $J/\psi$  in the LO of perturbative QCD as a function of the velocity of the quarkonium in QGP. To the LO, the elementary dissociation process is a thermal gluon dissociating the quarkonium into a  $c\bar{c}$  pair. Since the gluons acquire an effective thermal mass in the QGP, we introduce a constant thermal mass of either 400 or 600 MeV [39], respectively to represent a value at the lower and upper limit. The graphs in the left figure are obtained with a thermal gluon mass of 400 MeV, and the right figures with 600 MeV. The dissociation cross section in the LO has the maximum value when the absorbed energy is slightly above the threshold, and then rapidly decreases as the gluon energy increases further [33,34]. However, since the thermal mass of an absorbed gluon is larger than the energy that gives the maximum cross section, larger thermal mass will give smaller cross section. The binding energy of a  $J/\psi$  in QGP is obtained by solving the Schrödinger equation with a potential extracted from the lattice data, from which we find that it varies from 36.4 MeV to few keV as the temperature changes from  $1.13T_c$  to  $1.65T_c$  [30,35]. When the thermal mass of the absorbed gluon becomes larger, the dissociation begins at higher energy and the thermal width becomes smaller. This is why the thermal width with thermal gluon mass of 600 MeV is smaller than that with 400 MeV. The graphs at the LO also show that the thermal width decreases as the velocity of  $J/\psi$  in QGP increases. The reason for it is again simple to understand. As can be seen from Eq. (1), the thermal width is a convolution of elementary cross section, the relative velocity between the  $J/\psi$  and the colliding parton, and the thermal distribution function of the parton. However, as  $J/\psi$  moves across the parton matter, many slow partons becomes fast partons as seen by the  $J/\psi$ . As the dissociation cross section by fast parton is small in the LO, due to the small wave function overlap, the thermal width decreases.

The figures in the lower panel of Fig. 1 show the thermal width of  $J/\psi$  as a function of the velocity at the NLO, when the thermal mass of a parton is 400 MeV (left) or 600 MeV (right) respectively. These are the sum of quark induced and gluon induced NLO processes. As in the LO case, the width is smaller for larger thermal parton mass. This is mainly due to a larger virtuality of the gluon propagator when the initial parton has a larger thermal mass. As shown in the figure, in contrast to the results at the LO, the thermal widths slowly increase as the velocity of  $J/\psi$  increases. Such different behavior results from the asymptotic form of the NLO dissociation cross section, which converges to some finite value at the high energy limit. In Appendix A, we derive the asymptotic form of the NLO dissociation cross section, assuming the thermal parton mass to be sufficiently small. If the cross section is

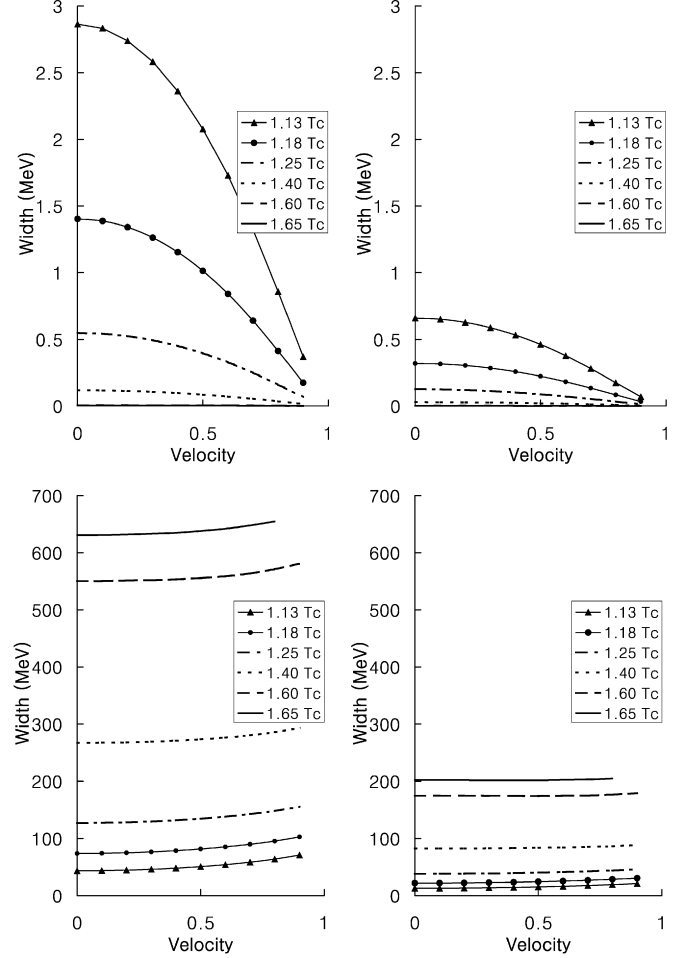


Fig. 1. The variation of the thermal widths  $\Gamma$  of  $J/\psi$  in the LO (upper) and in the NLO (lower) as a function of their velocity in QGP for various temperatures, and assuming the thermal mass of a parton to be 400 MeV (left) or 600 MeV (right).

almost constant, the thermal width can be approximated as follows,

$$\Gamma \sim \sigma \int \frac{d^3k}{(2\pi)^3} n(k_0) v_{\text{rel}}(\beta) \sim \langle v_{\text{rel}}(\beta) \rangle, \quad (5)$$

where  $\langle v_{\text{rel}}(\beta) \rangle$  is the expectation value of the relative velocity between partons and the  $J/\psi$  moving with velocity  $\beta$ . As mentioned above, as  $J/\psi$  moves faster, the expectation value of the relative velocity increases. If the  $J/\psi$  moves with the speed of light,  $\langle v_{\text{rel}}(\beta) \rangle$  approaches 1, and  $\Gamma \sim \sigma$ . In conclusion, while the width decreases in the LO, its magnitude is small such that the sum of the LO and the NLO width increases with the velocity.

Fig. 2 shows the thermal widths of  $\Upsilon$  as a function of its velocity in QGP. As in the case of  $J/\psi$ , the widths decrease in the LO, but increase in the NLO as the velocity increases. However, the slope of increase is steeper for  $\Upsilon$  than for the  $J/\psi$ , which comes from the difference in their binding energies. If the binding energy is larger, the threshold energy becomes larger and so does the energy at which the LO cross section becomes maximum. The dominant NLO process is a forward scattering

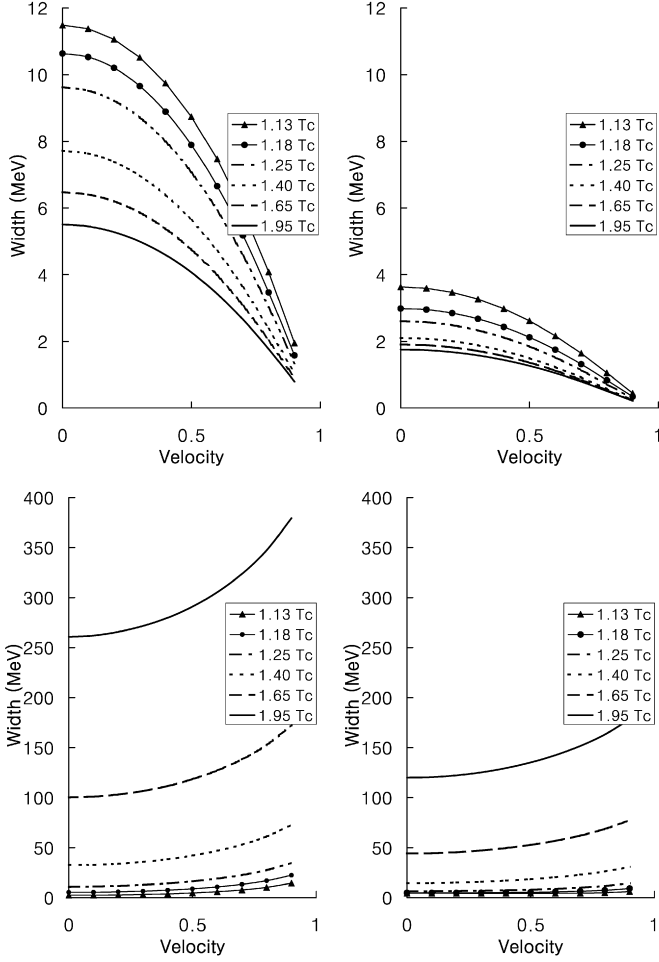


Fig. 2. The variation of the thermal width  $\Gamma$  of  $\Upsilon$  in the LO (upper) and in the NLO (lower) as a function of their velocity with the parton thermal mass of 400 MeV (left), of 600 MeV (right).

contribution, where the incoming parton emits a virtual gluon, which then dissociated the quarkonium via the LO process. This causes the monotonically increasing NLO cross section to reach its asymptotic value at a higher incoming energy when the binding energy is larger. This is the reason why for the  $\Upsilon$  system, the thermal width has a larger slope when the velocity increases. The thermal width steadily increases until the  $\Upsilon$  is traveling close to the speed of light so that most of the thermal partons have sufficient amount of energy to dissociate the  $\Upsilon$  at the asymptotic limit. In contrast, for the  $J/\psi$  at rest, nontrivial fraction of the thermal partons already dissociates the quarkonium at the asymptotic limit.

Up to now, the thermal mass of partons were assumed to be temperature independent for simplicity. However it is predicted to scale as  $g(T)T$  by finite temperature QCD calculations. Therefore, we finally present the result for the thermal widths of  $J/\psi$  and  $\Upsilon$  obtained with temperature dependent thermal masses for the partons. The masses of thermal gluon and quark are taken respectively as,

$$m_g^2(T) = \frac{g^2(T)T^2}{2} \left( \frac{N_c}{3} + \frac{N_f}{6} \right),$$

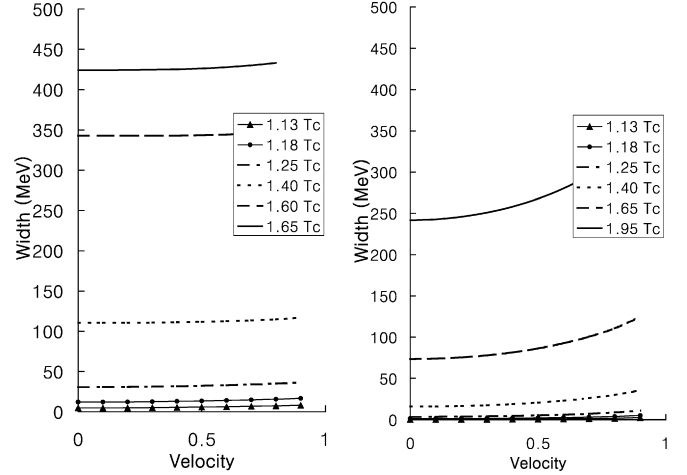


Fig. 3. The variation of the thermal width  $\Gamma$  of  $J/\psi$  (left) and of  $\Upsilon$  (right) from the sum of LO and NLO as a function of their velocity, obtained with the temperature dependent thermal mass [39].

$$m_q^2(T) = \frac{g^2(T)T^2}{3}, \quad (6)$$

with

$$g^2(T) = \frac{48\pi^2}{(11N_c - 2N_f) \ln F^2(T, T_c, \Lambda)}.$$

The number of color  $N_c$  is set to 3, and the number of flavor  $N_f$  to 3. For the function  $F(T, T_c, \Lambda)$ , we use the form obtained in [39] from a fit to the lattice QCD calculations. Fig. 3 shows the thermal widths of  $J/\psi$  and of  $\Upsilon$  obtained with temperature dependent parton masses. The magnitudes of the widths lie between the boundaries obtained with a constant thermal mass of 400 and 600 MeV, as shown in Figs. 1 and 2 for  $J/\psi$  and  $\Upsilon$ , respectively. This is so because the temperature dependent thermal mass lie between 400 and 600 MeV in the temperature range considered in this work. Moreover, the functional dependencies of the thermal widths with respect to the velocity are similar to those obtained with a constant thermal mass.

#### 4. Discussion

In the heavy ion collisions at LHC, not only will the heavy quarkonia be more amply produced, but be produced more energetically. The suppression and/or relative enhancement of these high  $p_T$  quarkonia will also occur in such an environment. In this respect, it is very important to know how the properties of heavy quarkonia will change when they move with respect to the QGP. Our result, based on the NLO perturbative QCD calculation, shows that the thermal width becomes larger as the quarkonium travels faster with respect to the QGP. The rate of increase is larger for the case of  $\Upsilon$  case than for the  $J/\psi$ , although the magnitude itself is larger for the latter. Our result suggests that the survival rate of  $J/\psi$  will be lower than that obtained with the velocity independent thermal width calculated at rest [30]. Consequently, if a relative suppression of  $J/\psi$  with higher than lower  $p_T$  is observed, as suggested by [25], it may be a consequence of the broadening of the thermal width of  $J/\psi$  as well as of the shortening of the Debye screening length.

The difference between these two effects is that the former depends on the size of fireball while the latter does not. Therefore, a systematic study on the A-dependence will be able to discriminate between these two effects.

### Acknowledgements

This work was supported by the Korea Research Foundation KRF-2006-C00011.

### Appendix A

Here, we derive the asymptotic form of the cross section for the process  $\Phi + q \rightarrow Q + \bar{Q} + q$  in high energy limit. The cross section for three-body decay is expressed as follow [30]

$$\sigma = \frac{g^4 m_Q^2 m_\Phi}{3\sqrt{(q \cdot k_1)^2 - m_\Phi^2 m_{k_1}^2}} \int_\alpha^\beta dw^2 \frac{\sqrt{1 - 4m_Q^2/w^2}}{16^2 \pi^3 m_\Phi |\vec{k}_1|} \times \int_{\alpha'}^{\beta'} dp_\Delta^2 \left| \frac{\partial \psi(\mathbf{p})}{\partial \mathbf{p}} \right|^2 \left( -\frac{1}{2} + \frac{k_{10}^2 + k_{20}^2}{2k_1 \cdot k_2} \right), \quad (\text{A.1})$$

where  $q, k_1, k_2$  are the momentum of quarkonium  $\Phi$ , incoming thermal quark, and outgoing thermal quark, respectively, and  $p_\Delta^2 = (k_1 - k_2)^2$ ,  $w^2 = (q + p_\Delta)^2$ . The momentum  $\mathbf{p}$  is the relative three momentum between  $Q$  and  $\bar{Q}$ . If the quarkonium is the Coulomb bound state of  $1S$ , the absolute square of derivative of quarkonium wavefunction is

$$\left| \frac{\partial \psi(\mathbf{p})}{\partial \mathbf{p}} \right|^2 = 2^{10} \pi a_0^5 \frac{a_0^2 \mathbf{p}^2}{(|a_0 \mathbf{p}|^2 + 1)^6} = 2^{10} \pi (a_0 \epsilon_0)^5 \frac{k_{10} - k_{20} - \epsilon_0}{(k_{10} - k_{20})^6}, \quad (\text{A.2})$$

where  $a_0$  is the Bohr radius and  $\epsilon_0$  is the binding energy of the quarkonium. In the second line of the above equation, the energy conservation condition  $m_\Phi + k_{10} = \mathbf{p}^2/m_Q + k_{20}$ , and the relation  $a_0^2 = 1/(\epsilon_0 m_Q)$  have been used. It might seem odd to use the nonrelativistic energy conservation condition in the high energy limit. However, in the high energy limit, the forward scattering is dominant, and therefore, while the incoming quark energy is very large, the transferred energy carried by the virtual gluon that dominantly dissociates the quarkonium is not large. This is so because the LO dissociation cross section is dominant near threshold. Hence a nonrelativistic treatment of the bound state kinematics is justified.  $\alpha, \beta, \alpha',$  and  $\beta'$  are the integration limits for drawing Dalitz plot on the plane of  $p_\Delta^2$  and  $w^2$ . They are respectively

$$\begin{aligned} \alpha &= 4m_Q^2, \\ \beta &= (\sqrt{s} - m_{k_1})^2, \\ \alpha' &= -b - \sqrt{b^2 - ac}, \\ \beta' &= -b + \sqrt{b^2 - ac}, \end{aligned} \quad (\text{A.3})$$

where

$$\begin{aligned} b &= \{s - (m_\Phi + m_{k_1})^2\} \{s - (m_\Phi - m_{k_1})^2\} / (2s) \\ &\quad - \{s - (m_\Phi^2 - m_{k_1}^2)\} (w^2 - m_\Phi^2) / (2s), \\ b^2 - ac &= \{(s - m_\Phi^2 + m_{k_1}^2)^2 - 4sm_{k_1}^2\} \\ &\quad \times \{w^2 - (u + m_{k_1})^2\} \{w^2 - (u - m_{k_1})^2\} / (4s^2). \end{aligned}$$

Here,  $s$  is the square of the initial energy in center-of-mass frame. In the limit of  $s \rightarrow \infty$ ,

$$\begin{aligned} \beta &\rightarrow s, \\ \alpha' &\rightarrow w^2 - s, \\ \beta' &\rightarrow 0, \\ k_{10}, |\vec{k}_1| &\rightarrow \frac{s}{2m_\Phi}, \\ k_{20} &\rightarrow \frac{s - w^2 + p_\Delta^2}{2m_\Phi} \end{aligned}$$

and the initial flux becomes

$$4\sqrt{(q \cdot k_1)^2 - m_\Phi^2 m_{k_1}^2} \rightarrow 2s. \quad (\text{A.4})$$

Then the elementary cross section becomes

$$\begin{aligned} \sigma &\approx \frac{16g^4 m_Q^2 m_\Phi (a_0 \epsilon_0)^5}{3\pi^2 s^2} \int_{4m_Q^2}^s dw^2 \sqrt{1 - \frac{4m_Q^2}{w^2}} \int_{w^2-s}^0 dp_\Delta^2 \\ &\quad \times \frac{(k_{10} - k_{20} - \epsilon_0)}{(k_{10} - k_{20})^6} \left[ -\frac{1}{2} + \frac{(k_{10} - k_{20})^2}{2k_1 \cdot k_2} + \frac{k_{10} k_{20}}{k_1 \cdot k_2} \right] \\ &\approx \frac{16g^4 m_Q^2 m_\Phi (a_0 \epsilon_0)^5}{3\pi^2 s^2} \int_{4m_Q^2}^s dw^2 \sqrt{1 - \frac{4m_Q^2}{w^2}} \int_{w^2-s}^0 dp_\Delta^2 \\ &\quad \times \frac{(k_{10} - k_{20} - \epsilon_0) k_{10} k_{20}}{(k_{10} - k_{20})^6 k_1 \cdot k_2}. \end{aligned} \quad (\text{A.5})$$

Because  $k_{10} - k_{20}$  varies from  $\epsilon_0$  approximately to  $s^{1/2}$ , first two terms in the square bracket have no contribution in the large  $s$  limit. After integration with respect to  $p_\Delta^2$ , the cross section becomes

$$\begin{aligned} \sigma &\approx \frac{2^8 g^4 m_Q^2 m_\Phi^4 (a_0 \epsilon_0)^5}{3\pi^2} \int_{4m_Q^2}^s dw^2 \\ &\quad \times \frac{\sqrt{1 - 4m_Q^2/w^2}}{(w^2 - m_\Phi^2)^5} \left[ -\frac{25}{12} + \ln \frac{w^2 - m_\Phi^2}{2m_{k_1}^2} \right. \\ &\quad \left. - \frac{2m_\Phi \epsilon_0}{w^2 - m_\Phi^2} \left( -\frac{137}{60} + \ln \frac{w^2 - m_\Phi^2}{2m_{k_1}^2} \right) \right], \end{aligned} \quad (\text{A.6})$$

where we used the following decomposition formula for integration with respect to  $p_\Delta^2$ ,

$$\begin{aligned} & \frac{1}{(x-a)(x-b)^n} \\ &= \frac{-1}{a-b} \frac{1}{(x-b)^n} + \frac{-1}{(a-b)^2} \frac{1}{(x-b)^{n-1}} + \dots \\ & \quad + \frac{-1}{(a-b)^n} \frac{1}{x-b} + \frac{1}{(a-b)^n} \frac{1}{x-a} \end{aligned}$$

and we ignored the thermal mass  $m_{k_1}$  for simplicity except in the logarithm as a regulator. This elimination brings about a potential problem when the binding energy is very small. To see its subtlety, consider the decomposition formula in the following example,

$$\begin{aligned} & \frac{1}{(2m_{k_1}^2 - p_\Delta^2)(w^2 - p_\Delta^2 - m_{J/\psi}^2)} \\ &= \frac{1}{w^2 - m_\Phi^2 - 2m_{k_1}^2} \left\{ \frac{1}{2m_{k_1}^2 - p_\Delta^2} - \frac{1}{w^2 - p_\Delta^2 - m_\Phi^2} \right\}. \end{aligned} \quad (\text{A.7})$$

Within the integration range, the left side of Eq. (A.7) is always positive. However, if the binding energy is very small,  $1/(w^2 - m_\Phi^2 - 2m_{k_1}^2)$  of the right side of Eq. (A.7) has a singularity. Of course, the term in the parenthesis on the right side diverges at the same time, and the equality is maintained. However, if the thermal mass  $2m_{k_1}^2$  is dropped during the approximation for simplicity, such divergence might not cancel and bring out the wrong result.

As the forward scattering becomes dominant in high energy scattering, most of the contributions come from the region  $w^2 \sim 4m_Q^2$  in the integration of  $w^2$ . Therefore, the main suppression factor in the integrand in Eq. (A.6) in the  $s \rightarrow \infty$  limit is  $1/(w^2 - m_\Phi^2)^5$ . Terms such as  $\ln(w^2 - m_\Phi^2)$  and  $1/\sqrt{w^2}$  can be replaced by  $\ln(4m_Q^2 - m_\Phi^2)$  and  $2m_Q$  respectively. Then we have,

$$\begin{aligned} \sigma &\approx \frac{2^7 g^4 m_Q m_\Psi^4 (a_0 \epsilon_0)^5}{3\pi^2} \int_{4m_Q^2}^s dw^2 \frac{\sqrt{w^2 - 4m_Q^2}}{(w^2 - m_\Phi^2)^5} \\ &\quad \times \left[ -\frac{25}{12} + \ln \frac{4m_Q^2 - m_\Phi^2}{2m_{k_1}^2} \right. \\ &\quad \left. - \frac{2m_\Phi \epsilon_0}{w^2 - m_\Phi^2} \left( -\frac{137}{60} + \ln \frac{4m_Q^2 - m_\Phi^2}{2m_{k_1}^2} \right) \right]. \end{aligned} \quad (\text{A.8})$$

Using the beta function

$$\int_0^\infty du \frac{u^m}{(1+u)^{m+n+2}} = \frac{m!n!}{(m+n+1)!},$$

the  $w^2$  dependent terms become

$$\begin{aligned} \lim_{s \rightarrow \infty} \int_{4m_Q^2}^s dw^2 \frac{\sqrt{w^2 - 4m_Q^2}}{(w^2 - m_\Phi^2)^5} &= \frac{5\pi}{128(4m_Q^2 - m_\Phi^2)^{7/2}}, \\ \lim_{s \rightarrow \infty} \int_{4m_Q^2}^s dw^2 \frac{\sqrt{w^2 - 4m_Q^2}}{(w^2 - m_\Phi^2)^6} &= \frac{7\pi}{256(4m_Q^2 - m_\Phi^2)^{9/2}}, \end{aligned}$$

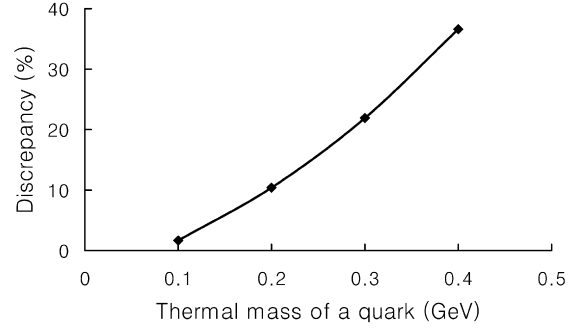


Fig. 4. The discrepancy between Eqs. (A.1) and (A.9).

and finally the cross section becomes

$$\begin{aligned} \sigma &\approx \frac{2g^4 m_\Phi^4 a_0^2}{3\pi m_Q^{1/2} (2m_Q + m_\Phi)^{9/2}} \left[ -\frac{125}{12} m_Q + \frac{167}{60} m_\Phi \right. \\ &\quad \left. + (5m_Q - m_\Phi) \ln \frac{\epsilon_0 (2m_Q + m_\Phi)}{2m_{k_1}^2} \right]. \end{aligned} \quad (\text{A.9})$$

Fig. 4 shows the discrepancy between the result of Eq. (A.1) and the result of Eq. (A.9) at  $\sqrt{s} = 100$  GeV, where we used the binding energy of  $J/\psi$  in the vacuum [34]. It is shown that the error decreases as the thermal mass of a parton decreases. If we further ignore the binding energy of a quarkonium,  $m_\Phi = 2m_Q$ , we find

$$\sigma \approx \frac{g^4 a_0^2}{48\pi} \left( 3 \ln \frac{2\epsilon_0 m_Q}{m_{k_1}^2} - \frac{97}{20} \right). \quad (\text{A.10})$$

This formula has several important features. First, the cross section is proportional to the square of the Bohr radius. It is a consequence of the dipole type of cross section, which is proportional to the derivative of the momentum wave function squared. The second important feature is the logarithmic term with argument proportional to the thermal mass, which acts as the regulator.

In the case of  $\Phi + g \rightarrow Q + \bar{Q} + g$ , the terms in the square bracket of Eq. (A.5) are replaced by the following [30,34]

$$\begin{aligned} & \frac{k_1 \cdot k_2}{k_{10} k_{20}} - 4 + \frac{2k_{10}}{k_{20}} + \frac{2k_{20}}{k_{10}} - \frac{k_{20}^2}{k_{10}^2} - \frac{k_{10}^2}{k_{20}^2} + \frac{2}{k_1 \cdot k_2} \\ & \quad \times \left[ (k_{10} - k_{20})^2 \left\{ \frac{(k_{10} + k_{20})^2}{k_{10} k_{20}} - 2 \right\} + k_{10} k_{20} \right]. \end{aligned} \quad (\text{A.11})$$

In the asymptotic limit, all but the last term in the square bracket of Eq. (A.11) are suppressed in the large  $s$  limit. Because its coefficient is twice of that for the quark induced case, the asymptotic cross section is two times larger. This ratio can also be seen in the quark and gluon induced dissociation cross sections shown in figures of Ref. [30].

We remark that the asymptotic value for the cross section obtained in Appendix A is for the Coulomb bound state, while in the previous sections, both the Bohr radius  $a_0$  and the binding energy  $\epsilon_0$  of quarkonia are extracted independently from lattice data, such that the relation  $a_0^2 = 1/(\epsilon_0 m_Q)$  is not satisfied. Moreover, the extracted binding energy is too small compared to the thermal mass of a parton, especially in the case of  $J/\psi$ .

Because of these reasons, Eq. (A.9) or Eq. (A.10) cannot be used directly. Nevertheless, the property that the dissociation cross section in the NLO converges to nontrivial finite value in the high energy limit is still maintained.

## References

- [1] T. Matsui, H. Satz, Phys. Lett. B 178 (1986) 416.
- [2] M.C. Abreu, et al., NA50 Collaboration, Phys. Lett. B 410 (1997) 327; M.C. Abreu, et al., NA50 Collaboration, Phys. Lett. B 410 (1997) 337; M.C. Abreu, et al., NA50 Collaboration, Phys. Lett. B 450 (1999) 456; M.C. Abreu, et al., NA50 Collaboration, Phys. Lett. B 477 (2000) 28.
- [3] M. Asakawa, T. Hatsuda, Y. Nakahara, Prog. Part. Nucl. Phys. 46 (2001) 459, hep-lat/0011040.
- [4] M. Asakawa, T. Hatsuda, Phys. Rev. Lett. 92 (2004) 012001, hep-lat/0308034.
- [5] S. Datta, F. Karsch, P. Petreczky, I. Wetzorke, Phys. Rev. D 69 (2004) 094507, hep-lat/0312037.
- [6] S. Datta, F. Karsch, P. Petreczky, I. Wetzorke, J. Phys. G 31 (2005) S351, hep-lat/0412037.
- [7] S. Datta, A. Jakovac, F. Karsch, P. Petreczky, AIP Conf. Proc. 842 (2006) 35, hep-lat/0603002.
- [8] R. Vogt, Acta Phys. Hung. A 25 (2006) 97, nucl-th/0507027.
- [9] T. Gunji, H. Hamagaki, T. Hatsuda, T. Hirano, hep-ph/0703061.
- [10] B. Alessandro, et al., NA50 Collaboration, nucl-ex/0612012.
- [11] B. Alessandro, et al., NA50 Collaboration, Eur. Phys. J. C 39 (2005) 335, hep-ex/0412036.
- [12] R. Arnaldi, et al., NA60 Collaboration, Nucl. Phys. A 774 (2006) 711.
- [13] P. Braun-Munzinger, J. Stachel, J.P. Wessels, N. Xu, Phys. Lett. B 344 (1995) 43, nucl-th/9410026.
- [14] P. Braun-Munzinger, J. Stachel, J.P. Wessels, N. Xu, Phys. Lett. B 365 (1996) 1, nucl-th/9508020.
- [15] F. Becattini, M. Gazdzicki, J. Sollfrank, Eur. Phys. J. C 5 (1998) 143, hep-ph/9710529.
- [16] P. Braun-Munzinger, I. Heppe, J. Stachel, Phys. Lett. B 465 (1999) 15, nucl-th/9903010.
- [17] P. Braun-Munzinger, D. Magestro, K. Redlich, J. Stachel, Phys. Lett. B 518 (2001) 41, hep-ph/0105229.
- [18] P. Braun-Munzinger, J. Stachel, Phys. Lett. B 490 (2000) 196, nucl-th/0007059.
- [19] R.L. Thews, J. Phys. G 32 (2006) S401, and references cited therein.
- [20] A. Andronic, P. Braun-Munzinger, K. Redlich, J. Stachel, Phys. Lett. B 652 (2007) 259, nucl-th/0701079.
- [21] L. Grandchamp, R. Rapp, G.E. Brown, Phys. Rev. Lett. 92 (2004) 212301, hep-ph/0306077.
- [22] L. Yan, P. Zhuang, N. Xu, Phys. Rev. Lett. 97 (2006) 232301, nucl-th/0608010.
- [23] K. Morita, S.H. Lee, arXiv: 0704.2021 [nucl-th].
- [24] Y. Kim, J.P. Lee, S.H. Lee, Phys. Rev. D 75 (2007) 114008, hep-ph/0703172.
- [25] H. Liu, K. Rajagopal, U.A. Wiedemann, Phys. Rev. Lett. 98 (2007) 182301, hep-ph/0607062.
- [26] D. Cabrera, R. Rapp, hep-ph/0611134.
- [27] W.M. Alberico, A. Beraudo, A. De Pace, A. Molinari, Phys. Rev. D 75 (2007) 074009, hep-ph/0612062.
- [28] W.M. Alberico, A. Beraudo, A. De Pace, A. Molinari, arXiv: 0706.2846 [hep-ph].
- [29] A. Mocsy, P. Petreczky, arXiv: 0705.2559 [hep-ph]; A. Mocsy, P. Petreczky, arXiv: 0706.2183 [hep-ph].
- [30] Y. Park, K.I. Kim, T. Song, S.H. Lee, C.Y. Wong, Phys. Rev. C 76 (2007) 044907, arXiv: 0704.3770 [hep-ph].
- [31] M.E. Peskin, Nucl. Phys. B 156 (1979) 365.
- [32] G. Bhanot, M.E. Peskin, Nucl. Phys. B 156 (1979) 391.
- [33] Y.S. Oh, S. Kim, S.H. Lee, Phys. Rev. C 65 (2002) 067901, hep-ph/0111132.
- [34] T. Song, S.H. Lee, Phys. Rev. D 72 (2005) 034002.
- [35] C.Y. Wong, Phys. Rev. C 72 (2005) 034906, hep-ph/0408020.
- [36] M.C. Chu, T. Matsui, Phys. Rev. D 39 (1989) 1892.
- [37] M.G. Mustafa, M.H. Thoma, P. Chakraborty, Phys. Rev. C 71 (2005) 017901.
- [38] M. Chernicoff, J.A. Garcia, A. Guijosa, JHEP 0609 (2006) 068, hep-th/0607089.
- [39] P. Levai, U.W. Heinz, Phys. Rev. C 57 (1998) 1879, hep-ph/9710463.